ACS SENSORS

Article

pubs.acs.org/acssensors

Structure Guided Design of Protein Biosensors for Phenolic Pollutants

Shamayeeta Ray,[†] Santosh Panjikar,[‡,§] and Ruchi Anand*[,∥,⊥]

[†]IITB-Monash Research Academy, Mumbai 400076, Maharashtra, India

[‡]Department of Biochemistry and Molecular Biology, Monash University, Clayton, Victoria 3800, Australia

[§]Australian Synchrotron, Clayton, Victoria 3168, Australia

[∥]Department of Chemistry, Indian Institute of Technology Bombay, Mumbai 400076, Maharashtra India

[⊥]Wadhwani Research Center for Bioengineering, IIT Bombay, Mumbai 400076, India

Supporting Information

ABSTRACT: Phenolic aromatic compounds are a major source of environmental pollution. Currently there are no in situ methods for specifically and selectively detecting these pollutants. Here, we exploit the nature's biosensory machinery by employing *Acinetobacter calcoaceticus* NCIB8250 protein, MopR, as a model system to develop biosensors for selective detection of a spectrum of these pollutants. The X-ray structure of the sensor domain of MopR was used as a scaffold for logic-based tunable biosensor design. By employing a combination of in silico structure guided approaches, mutagenesis and isothermal calorimetric studies, we were able to generate biosensor templates, that can selectively and specifically sense harmful compounds like chlorophenols, cresols, catechol, and xylenols. Furthermore, the ability of native protein to selectively sense phenol as the primary ligand was also enhanced. Overall, this methodology can be extended as a suitable framework for development of a series of exclusive biosensors for accurate and selective detection of aromatic pollutants from real time environmental samples.

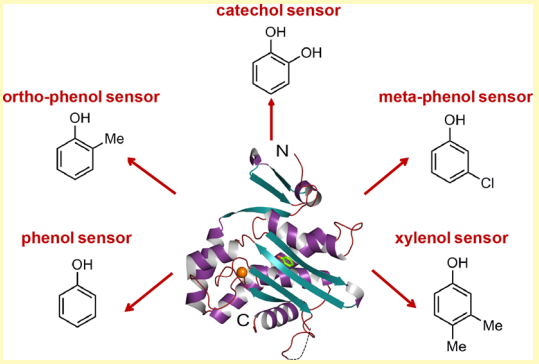

KEYWORDS: *NtrC, MopR, phenol, catechol, xylenols, 3-chlorophenol, selective biosensor*

The phenolic class of xenobiotics like chlorophenols, catechol, dimethylphenols, and cresols are major pollutants generated by oil, paper, tannery, and several other industries[1] and are listed as toxic and priority pollutants in the United States Environmental Protection Agency (EPA) and world pollution databases. Some of these compounds like bulkier dimethylphenols are resistant to biodegradation and have half-lives extending for several years in the environment.[2] These xenobiotics enter the soil and water bodies as waste and become dangerous if leaked into drinking water sources as they are extremely embryotoxic and carcinogenic in nature.[3] The current methods to detect these phenolic compounds rely on liquid−liquid extraction followed by gas chromatography, flame ionization detection, and tandem mass spectrometry.[4,5] However, these methods are time-consuming and require an elaborate instrumentation setup. Hence, there is a dire need to develop methodologies that can accurately, quickly and with high sensitivity detect these pollutants in real time. Devising chemical strategies that can differentiate between ligands like cresols, phenol, catechol, and disubstituted phenols is a daunting task, mostly because these classes of compounds are by and large inert to detection. Hence, exploiting nature's biosensory machinery that has been subject to evolutionary rigor, pose as a viable alternative. Prokaryotic soil bacteria like *Pseudomonas* sp. offer an excellent strategy toward developing cost-effective biosensors for the said pollutants.[6,7] These bacteria possess special regulatory systems, which when faced with adversity are capable of detecting specific pollutant molecules and degrading them.[8−10] The degradative pathways are either integrated into their host genome or are in the form of an entire gene cassette, helper plasmids.[11] The expression of these catabolic aromatic gene clusters is under the tight control of highly regulated transcription factors, like the nitrogen regulating class (NtrC) of proteins.[11,12]

NtrC regulators like XylR, DmpR, and MopR consist of three major domains, the N-terminal pollutant sensing domain (A), the AAA+ ATPase readout domain (C), and a C-terminally located DNA binding domain (D)[13,14] (Figure 1A). The A and the C domains are connected by a flexible helical linker designated as B linker[15] (Figure 1A). Biochemical experiments have shown that, in the absence of the aromatic pollutants, the ATPase activity of the central AAA+ (C) domain remains repressed and activation occurs only upon binding of the target pollutants to the signal reception (A) domain.[16,17] Thus, it

Received: December 27, 2016
Accepted: February 22, 2017
Published: February 22, 2017

DOI: 10.1021/acssensors.6b00843
ACS Sens. XXXX, XXX, XXX−XXX

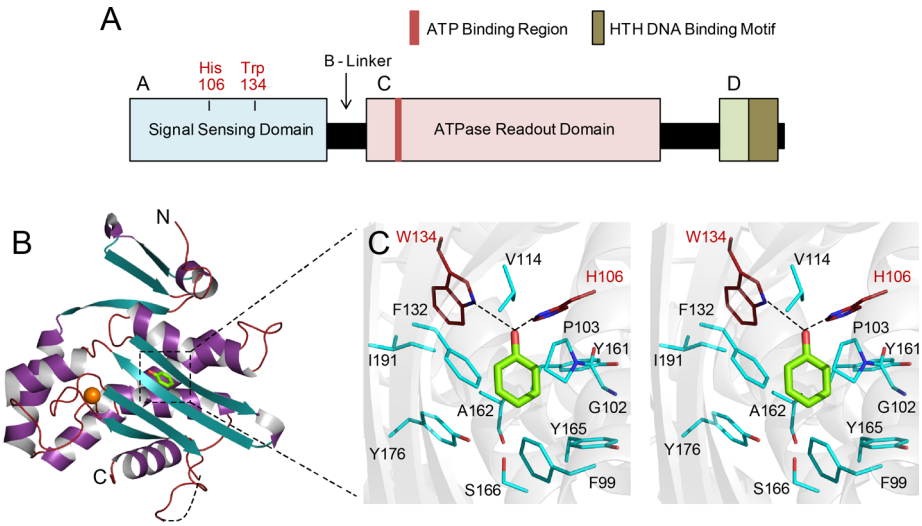

Figure 1. Structural insights into the pollutant sensing domain of MopR. (A) Domain organization of MopR, an NtrC family regulator.[22] Site-specific mutations have been carried out on the signal sensing anchors (listed in red) in the pollutant sensing (A) domain (colored light blue) of MopR. (B) Crystal structure of the pollutant sensing (A) and linker (B) domain of MopR (MopR^{AB}) nesting a zinc atom (in orange) and a bound phenol (in green).[22] [Panels (A) and (B) have been adapted in part from ref 22. Copyright 2016 American Chemical Society.] (C) Magnified stereo view of the pollutant binding pocket of MopR^{AB} as obtained from the phenol-bound crystal structure. The two sensor residues W134 and H106 anchoring the phenolic OH are in firebrick and the other ligand-binding residues are in cyan. Oxygen and nitrogen atoms are in red and blue, respectively.

appears that this sensing design of these regulators can serve as an excellent platform for biosensor development, as both signal reception and readout domain exist within the same protein system.

Over the past few decades, several attempts have been made to develop effective biosensors for an array of xenobiotics using this subclass of regulators.[18,19] However, most of these targets were difficult to achieve due to lack of knowledge of the actual sensor determinants.[20,21] In the absence of any X-ray structure for this family, most of the mutations in the past were performed using various in silico models and via domain shuffling techniques.[20,21] Earlier this year, there was a breakthrough in the field where Ray et. al successfully solved the crystal structure of the signal sensing (A) and linker (B) domain of a protein from this subfamily, MopR (MopR^{AB}), in complex with phenol and its derivatives[22] (Figure 1B, PDB code: 5KBE). In parallel, Patil et al. also solved the structure of the phenol sensing domain of PoxR, a close analogue of MopR.[23] The crystal structure of MopR^{AB} holds several surprises; although the protein is of bacterial origin, it resembles eukaryotic proteins and possess a fold similar to nitric oxide signaling and golgi transport enzymes that harbor long chain fatty acids molecules.[24] The MopR protein also contains a novel zinc binding motif that does not play any role in sensing, however, imparts overall structural stability. The structure reveals that the pollutant is nested in a hydrophobic pocket lined by residues like phenylalanine, isoleucine, alanine and tyrosine with the phenolic ligand being anchored by the indole nitrogen atom of W134 and the imidazole nitrogen atom of H106 (Figure 1C). Moreover, supporting isothermal calorimetry (ITC) data shows that native MopR binds only small phenolic ligands and is unable to tolerate much variation in ligand architecture (Figure 5B; Table S2).[22]

Armed with the structural information, here we used the ligand binding pocket as a template to expand its sensing repertoire and to create several specific biosensor models for selective sensing of toxic environmental pollutants like hazardous air pollutant catechol, highly corrosive pollutants 3-chlorphenol (3-cp) and cresols, toxic aquatic pollutants xylenols and priority pollutant phenol. The substrate scope was altered by employing targeted mutagenesis as the primary tool. The design of the mutations was first refined by in silico mutagenesis along with docking studies and a recombinant MopR-aromatic pollutant pair for each mutation was identified. The in silico results were corroborated by carrying out the select mutations, purifying the proteins and performing ITC based binding profile characterizations of the different pollutant-MopR^{AB} mutant combinations. The biosensor design was further substantiated by augmenting the ATPase readout (C) domain to different MopR^{AB} variants and creating MopR^{ABC} mutants that served as a sensing chimera for direct pollutant readout down to low ppm levels. Together, this structure based approach provides enhanced selectivity and represents an appropriate scaffold for development of a series of selective and exclusive biosensors for a host of hazardous environmental pollutants.

EXPERIMENTAL SECTION

Docking Studies. Based on the detailed analysis of the different aromatic pollutant bound structures of the signal sensing (A) domain along with part of the linker region (B) of MopR (MopR^{AB}),[22] various site-specific mutations of the two major phenol binding residues H106 and W134 were designed in silico (Figure 1A). Docking experiments were performed using AutoDock version 4.2[25] with the mutated constructs to test for any alterations in specificity and selectivity of the substrate scope of MopR^{AB} (Table S1). The mutations included (i) alanine substitutions, MopR$^{AB}_{HA}$ (H106A substitution), MopR$^{AB}_{WA}$ (W134A substitution), and MopR$^{AB}_{WHA}$ (W134A-H106A double mutation), (ii) asparagine substitution MopR$^{AB}_{HN}$ (H106N substitution) and (iii) tyrosine substitution of H106, MopR$^{AB}_{HY}$ (H106Y substitution), and they were docked with the following select phenolic pollutants: phenol, *o*-cresol, *m*-cresol, catechol, 3-chlorophenol (3-cp), and 3,4-dimethylphenol (3,4-dmp) (Figure 5A; Table S1) (detailed in Supporting Materials and Methods).

DNA Manipulations, Overexpression, and Purification of the Recombinant Proteins. To validate the docking results, the same set

DOI: 10.1021/acssensors.6b00843
ACS Sens. XXXX, XXX, XXX−XXX

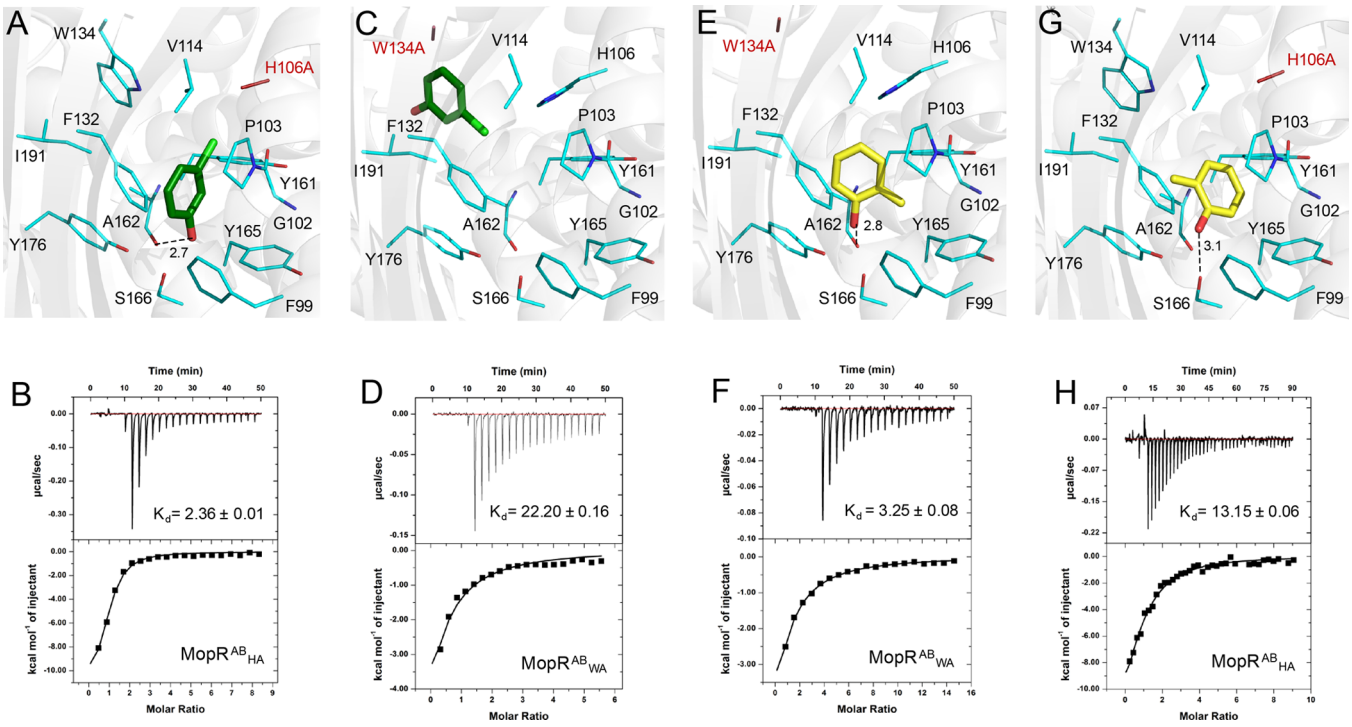

Figure 2. Selective sensing of *ortho* and *meta* directed phenolic pollutants. Panels represent docked ligands and the ITC curves for the following MopR^{AB} mutants (A,B) 3-cp with MopR$^{AB}_{HA}$, (C,D) 3-cp with MopR$^{AB}_{WA}$, (E,F) *o*-cresol with MopR$^{AB}_{WA}$, and (G,H) *o*-cresol with MopR$^{AB}_{HA}$. Pocket residues are in cyan and mutated residues in firebrick. Oxygen and nitrogen atoms are in red and blue, respectively. The ITC data corresponding to each docking experiment is given in the panels below. ITC data were fit using one set of sites model and the thermodynamic parameters are given in Table S2. All the K_d values represented in the figure are in μM.

of in silico mutations were experimentally incorporated into the native MopR^{AB} construct from *Acinetobacter calcoaceticus* NCIB8250 that was previously cloned into modified pET vector.[22] Further, to test the translational biosensing ability of the different MopR^{AB} sensor designs, a longer construct of the native MopR (MopR^{ABC}) consisting of both the signal sensing (A and B) and the readout ATPase (C) domain, was cloned into modified pET vector (Figure 1A). The native MopR^{ABC} was then used as a template to perform following mutations within the bigger construct - MopR$^{ABC}_{HY}$ (H106Y substitution), MopR$^{ABC}_{HN}$ (H106N substitution) and MopR$^{ABC}_{HA}$ (H106A substitution). All the point mutations in MopR^{AB} and MopR^{ABC} were performed by employing standard site-directed mutagenesis protocol using the "site-directed mutagenesis kit" from Kapa biosystems. The native as well as the mutated protein constructs were expressed as His-tag fusion proteins and were purified using standard His-tagged affinity purification protocol (detailed in Supporting Materials and Methods).

Ligand Binding Experiment Using ITC. In order to validate the in silico affinity of different MopR^{AB} mutants toward selective phenolic pollutants, in vitro ligand binding experiments were performed using a MicroCal iTC200 instrument (GE Healthcare, WI) (detailed in Supporting Materials and Methods, Table S2).

Colorimetric ATPase Assay Design. The biosensing ability of native and mutated MopR^{ABC} toward a variety of aromatic pollutants were tested using malachite green based colorimetric ATPase assay[26] and monitored spectrophotometrically at 630 nm (details of assay protocol provided in Supporting Materials and Methods).

RESULTS AND DISCUSSION

In order to create modified sensor designs by employing the structure as a template, a series of pollutant targets ranging from phenol, xylenols and catechol were chosen. The first set of biosensors were designed to be specific toward *ortho* and *meta* substituted phenolic ligands like *o*-cresol and 3-cp, respectively. The native structure clearly reveals that both these pollutants snugly fit into the binding pocket in a fixed conformation with little room for reorientation or for accepting any extra side groups.[22] Therefore, to alter the substrate scope in favor of *meta* and *ortho* directed aromatics, one strategy that was undertaken was to create space in the pocket. To do so, only one of the phenolic anchors H106 or W134 was retained and other was mutated to an alanine residue. This would ensure additional free movement that can enable the differently directed ligands to be selectively accommodated. To test this hypothesis, in silico mutations involving single alanine substitution of the key sensor residues MopR$^{AB}_{HA}$ (H106A) and MopR$^{AB}_{WA}$ (W134A) were constructed. Docking MopR$^{AB}_{HA}$ and MopR$^{AB}_{WA}$ with a subset of *meta* and *ortho* substituents revealed that MopR$^{AB}_{HA}$ preferred meta-substituted effectors, whereas MopR$^{AB}_{WA}$ favored *ortho* directed compounds (Figure 2). This is because, in MopR$^{AB}_{HA}$, the *meta* directed compounds are able to flip in the active site and the phenolic OH now instead of anchoring with W134, forms strong hydrogen bond with the carbonyl group of residue A162. The binding affinity in this conformation is likely to be retained as the ligand still fits into the pocket in a favorable orientation with its *meta* directed group accommodating itself in the space created by the lack of histidine residue (Figure 2A). Similarly, *ortho*-substituted ligands prefer MopR$^{AB}_{WA}$ mutant as again, due to the shape complementarity, the ligand is able to flip and interact with the backbone of A162 through hydrogen bonding interactions with the main chain carbonyl group without any steric clash (Figure 2E). Docking also shows that the MopR$^{AB}_{WA}$ mutation is unfavorable toward *meta* directed ligands as these compounds are neither able to flip in the pocket, due to a steric clash of the *meta*-directed substituent of the flipped ligand with H106, nor maintain the original

DOI: 10.1021/acssensors.6b00843
ACS Sens. XXXX, XXX, XXX−XXX

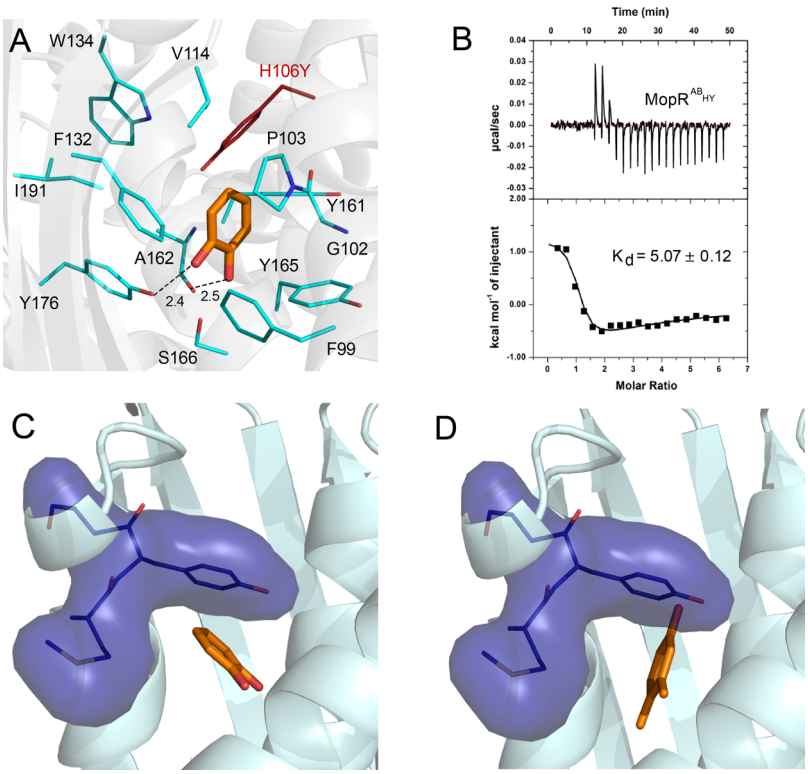

Figure 3. Selective catechol sensor design. Panels (A) and (B) represent docked catechol and the ITC curve for MopR$^{AB}_{HY}$ mutant, respectively. Panels (C) and (D) show the surface representation of the MopR$^{AB}_{HY}$ binding pocket with catechol and 3,4-dmp, respectively. Carbon atoms of all the phenolic ligands are colored orange, pocket residues are in cyan and mutated residues in firebrick. The surface representation of the tyrosine side chain is in deep blue. Oxygen and nitrogen atoms are in red and blue, respectively. ITC data was fit using one set of sites model and the thermodynamic parameters are given in Table S2. K_d values represented in the figure are in μM.

conformation (Figure 2C). Instead, the *meta*-oriented compound occupies the empty space created by the W134A mutation adopting a conformation approximately 7 Å away from the original optimal position. Similarly, MopR$^{AB}_{HA}$ docked with o-cresol shows that it does not favor ligands with *ortho* substitutions as the phenolic OH group comes in close proximity of another electron donating S166-OH (Figure 2G), an energetically unfavorable scenario. Experimental results with purified mutants (Supporting Materials and Methods) corroborate the in silico predictions. The binding affinity (K_d) of these mutants showed that MopR$^{AB}_{HA}$ prefers meta-substituted phenols over their *ortho* directed counterparts by over 10-fold (Figures 2B,H, 5B, and S1; Table S2). An opposite trend in binding affinity was observed for the MopR$^{AB}_{WA}$ mutation where *ortho* oriented compounds bind with much higher affinity than their *meta* directed counterparts (Figures 2D,F, 5C, and S2; Table S2). Hence, engineering the binding pocket with these alanine substitutions have led to creation of sensor frameworks with enhanced selectivity toward *ortho*- or *meta*-substituted phenolic pollutants.

Our next goal was to generate an exclusive sensor for catechol, a water-soluble, volatile skin and eye irritant, which acts as a central nervous system depressant and can cause hypertension and convulsions. Since catechol can easily enter the water sources, there is a dire need to monitor its levels. Our *ortho* directed study revealed that catechol being bulky with two hydroxyl groups might fit better in a flipped orientation. To facilitate the flip, the suggested design would have the histidine position blocked with an alternative amino acid with the anchor properties obliterated. The tyrosine residue having an aromatic hydroxyl group, fits the above-mentioned parameters, hence an in silico MopR$^{AB}_{HY}$ (H106Y) mutation was performed. Docking results were extremely encouraging; the flipped catechol adopted a favorable conformation without any steric clash (Figure 3C). In this conformation, one of its OH moieties makes a strong hydrogen bond with the carbonyl group of A162 and the other OH interacts with Y176 leading to further stabilization (Figure 3A). Docking with all other phenol derivatives, however, resulted in unfavorable orientations producing no logical contacts with the MopR$^{AB}_{HY}$ pocket residues (Figure 3D). Experimental validation of MopR$^{AB}_{HY}$ again confirms the predictions and reveals that phenol and most of the other phenolic effectors, exhibit extremely poor affinity toward MopR$^{AB}_{HY}$ (Figures 5G and S3; Table S2). The only exception was catechol that showed substantial affinity (K_d of 5.07 $\pm$ 0.12 μM) (Figures 3B and 5G; Table S2). These results indicate that MopR sensor binding pocket is extremely sensitive to single point changes, and a sole mutation can completely alter the binding profile of the sensor protein. Thus, the MopR$^{AB}_{HY}$ mutant is selective for stabilization of catechol, providing a framework to design an exclusive catechol sensor.

Xylenols (bulkier phenols), like dimethylphenols, are long lasting aquatic pollutants that enter the environment through processes like production of phenolic resins commonly used for poly(*p*-phenylene oxide), antioxidants, and varnishe production. In order to develop selective sensors for these xylenols, the current aim was to increase the pocket size while retaining the phenolic anchor. It was noticed from studies on the previous sensors (MopR$^{AB}_{HY}$, MopR$^{AB}_{HA}$) that an effective strategy was to use A162 as a phenolic anchor and flip the

DOI: 10.1021/acssensors.6b00843
ACS Sens. XXXX, XXX, XXX−XXX

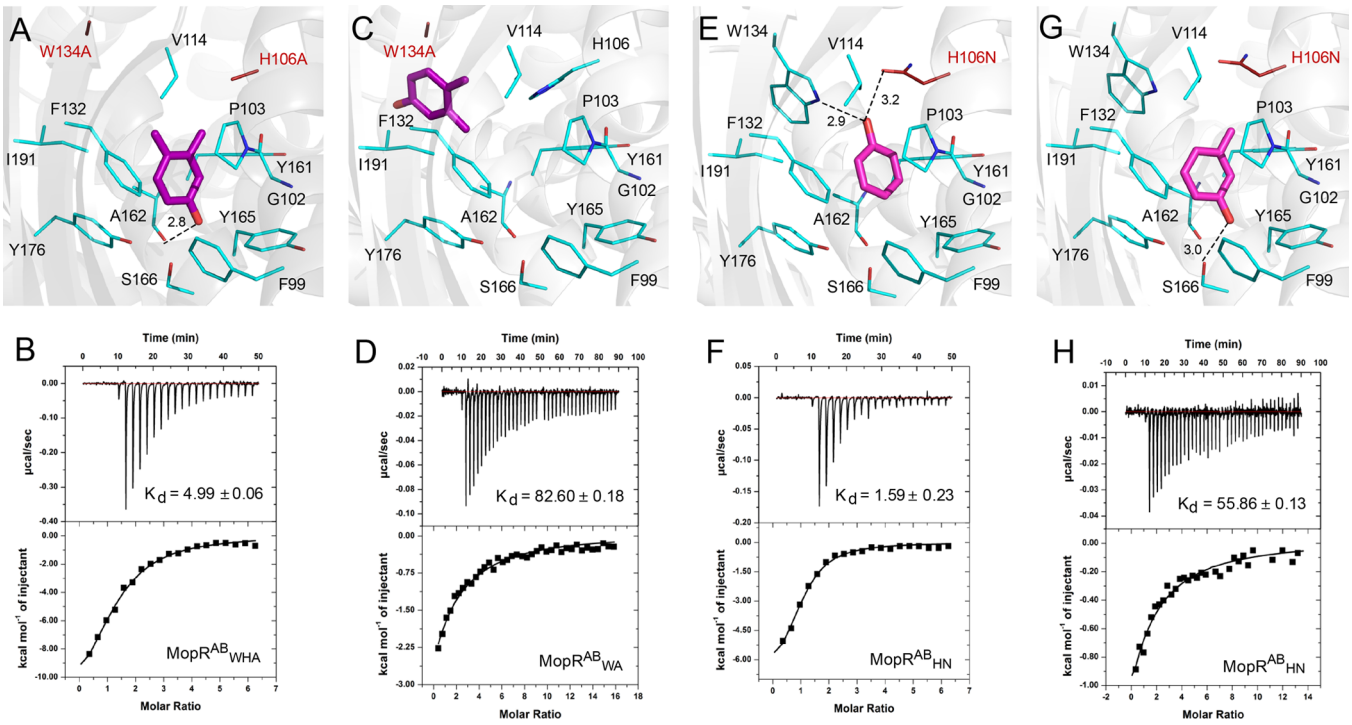

Figure 4. Selective sensing of xylenols and phenol. The panels represent docked ligands and the ITC curves for the following MopR^{AB} mutants: (A,B) 3,4-dmp with MopR$^{AB}_{WHA}$, (C,D) 3,4-dmp with MopR$^{AB}_{WA}$, (E,F) phenol with MopR$^{AB}_{HN}$, and (G,H) *m*-cresol with MopR$^{AB}_{HN}$. Pocket residues are in cyan and mutated residues in firebrick. Oxygen and nitrogen atoms are in red and blue, respectively. The ITC data corresponding to each docking experiment is given in the panels below. ITC data were fit using one set of sites model and the thermodynamic parameters are given in Table S2. All the K_d values represented in the figure are in μM.

alcohol. Hence, an adaptive design with increased pocket volume was created in silico that involves a double alanine substitution of both W134 and H106 residues generating the MopR$^{AB}_{WHA}$ (W134A-H106A) construct design. The docking studies with one of the xylenols, 3,4-dimethylphenol(3,4-dmp), shows that it flips in the MopR$^{AB}_{WHA}$ pocket in an orientation as predicted, with the OH group making strong hydrogen bonding interaction with the main chain carbonyl group of A162. The double alanine substitution creates sufficient space in the pocket to accommodate both the methyl groups of 3,4-dmp in favorable conformation without any steric clash leading to an overall stabilized state (Figure 4A). In contrast, single mutants like MopR$^{AB}_{HA}$, MopR$^{AB}_{WA}$ and MopR$^{AB}_{HN}$ (H106N) could not create enough space to allow a proper anchoring of 3,4-dmp (Figures 4C and S4A,C). The ITC results clearly reasserts the observations from docking as 3,4-dmp has the highest affinity for the MopR$^{AB}_{WHA}$ mutant (K_d of 4.99 ± 0.06 μM) (Figure 4B, 5E, Table S2) and shows extremely poor affinity or almost no binding toward the other single mutants (Figures 4D and S4B,D; Table S2). MopR$^{AB}_{WHA}$ also shows some affinity toward other *meta*-directed bulkier phenol derivatives like 3-cp and m-cresol (Figures S5 and 5E; Table S2) but their affinity is much less compared to 3,4-dmp. Based on all these observations, it can be inferred that MopR$^{AB}_{WHA}$ can serve as a model construct for selective sensing of bulkier toxic aromatic pollutants. These results reflect that logic-based tweaking of the MopR binding pocket can indeed help in sensing new effectors which are usually weak binders of the native protein.

Although the native protein senses phenol with high affinity, it exhibited some level of promiscuity. Hence, we shifted our focus on improving the phenol sensing design of the native MopR. This will aid in exclusive detection of phenol without any background signal from other alcohols. To facilitate this, a design tailored to conformationally constrict the phenolic anchor will be the most suited. Therefore, the anchor H106 was replaced with an asparagine residue which has a similar size and pK_a value (approximately ~9) like the delta nitrogen of histidine residue, but adopts specific rotamers in the pocket. In silico H106N substitution (MopR$^{AB}_{HN}$) shows that only phenol can be effectively docked in the MopR$^{AB}_{HN}$ binding pocket as compared to all other phenol derivatives (Figures 4E,G and S6A,C). Docking further shows that the OH group of the phenol retained the hydrogen bond with W134 along with formation of a new bond with N106 leading to an overall stabilization of the ligand (Figure 4E). However, for *o*-cresol (having the methyl group at the *ortho* positon), it was observed that the ligand rotated in a manner where it could make hydrogen bond with only W134 and not N106 leading to weaker interactions (Figure S6A). In case of *m*-cresol and catechol, both the ligands flipped within the MopR$^{AB}_{HN}$ pocket and their OH groups could make only weak hydrogen bonds with Y176-OH and S166-OH leading to overall destabilization (Figures 4G and S6C). In vitro ligand binding experiments of MopR$^{AB}_{HN}$ validated the docking results, where only phenol exhibited high affinity (K_d of 1.59 ± 0.23 μM) (Figure 4F) and all the other phenol derivatives showed poor affinity toward MopR$^{AB}_{HN}$ (Figures 4H, S6B,D, and 5F; Table S2). Though the affinity of MopR$^{AB}_{HN}$ toward phenol is slightly reduced as compared to the native protein (K_d of 0.46 ± 0.06) (Table S2) but the advantage of this mutation lies in the fact that it can now selectively sense phenol over other pollutants, a property which is lacking in native MopR^{AB} (Figure 5B, F). These observations highlight the importance of correct choice of

DOI: 10.1021/acssensors.6b00843
ACS Sens. XXXX, XXX, XXX−XXX

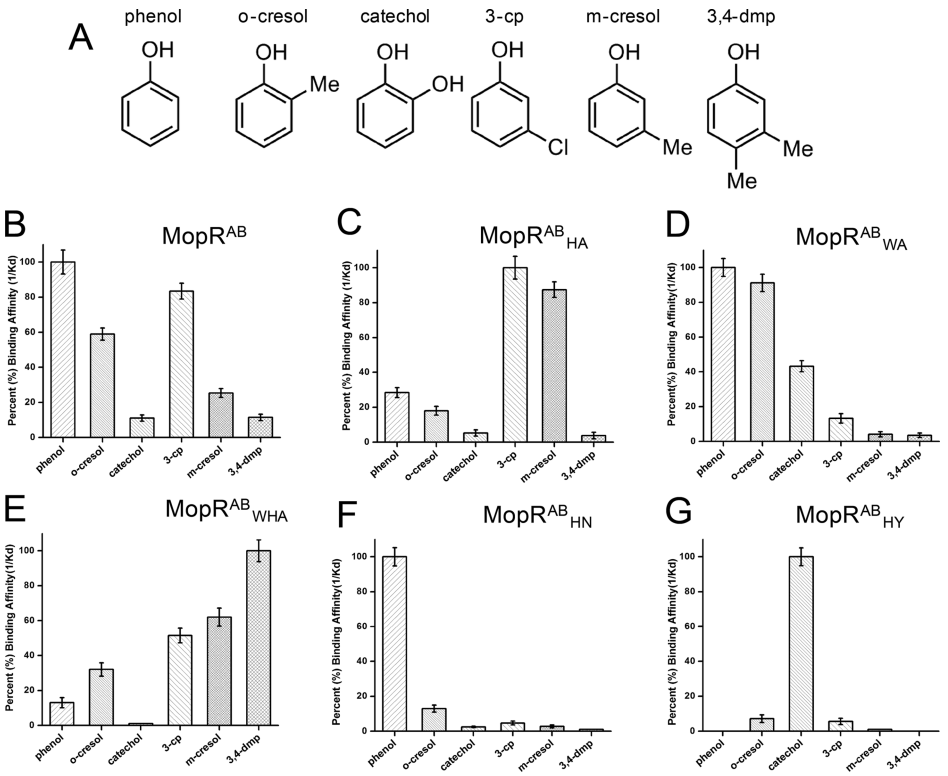

Figure 5. Binding affinity of MopR^{AB} and its mutants toward different phenol derivatives. Panel (A) represents structures of the aromatic compounds. Panels (B)−(G) represent the affinity of various MopR^{AB} constructs toward different phenol derivatives based on the K_d values obtained from the ITC data of each ligand-protein run (Table S2). The *Y*-axis in each bar diagram represents percent (%) binding affinity (computed based on $1/K_d$) for each ligand. The compounds for which K_d values are "not determinable" have been assigned value of 1 and represent those ITC runs for which some heat change was observed but the data could not be fit using any standard binding curve models and hence, their thermodynamic parameters could not be computed. "No binding" refers to those ITC runs where there was negligible heat change and, hence, have been assigned value of 0 in the bar plots shown above.

amino acids in the active site and assert the fact that substitution of any hydrophilic amino acid with another capable of hydrogen bonding is not sufficient to anchor a wide spectrum of phenolic pollutants within the MopR pocket.

To demonstrate that the designed model systems can be directly translated as biosensor units, longer constructs of MopR consisting of both the signal sensing(A) (pollutant binding) and the readout(C) (ATP hydrolysis) domain (Figure 1A) for the native (MopR^{ABC}) as well as three single mutants, MopR$^{ABC}_{HA}$ (H106A, corresponding to the *meta*-phenol sensor model), MopR$^{ABC}_{HY}$ ((H106Y, corresponding to the catechol sensor model) and MopR$^{ABC}_{HN}$ ((H106N, corresponding to the phenol sensor model) were constructed and purified. The ATPase activity of both native and mutated MopR^{ABC} which gets activated on target pollutant binding to the sensing domain, was quantified by colorimetric estimation.[26] Assay with each protein construct was performed with a host of simulated wastewater samples, each containing a different aromatic pollutant as the primary contaminant (Figure 5A). To confirm viability of the design, each of the pollutant's concentration used for testing were set at 10 μM (corresponding to 0.94 ppm for phenol, 1.1 ppm for catechol, 1.08 ppm for *m*-cresol and *o*-cresol, 1.28 ppm for 3-cp, and 1.22 ppm for 3,4-dmp) which lies below the approximate environmental risk limits as per the Occupational Safety and Health Administration (OSHA). Results show that each MopR^{ABC} mutant protein exhibited significant ATPase activity only toward those compounds for which that particular MopR^{AB} construct has high affinity (Figure 6B−D), thereby validating our docking and ITC studies. Hence, native MopR^{ABC} displayed a broader sensing spectrum (Figure 6A), whereas the mutants behaved as selective biosensors (Figure 6B−D). Similar translational biosensing responses are expected for the other sensor designs. Therefore, these selective sensors pave the way toward design of biosensing tools to gauge levels of particular contaminants in wastewater environmental samples and to categorize the type of pollutants present in them.

CONCLUSION

In summary, the in silico as well as experimental analysis of various phenolic pollutants with the different MopR variants highlight the fact that structure guided protein engineering of the binding pocket can help generate selective biosensors that can be designed to possess enhanced ability to target one or more hazardous aromatic pollutants. The efficient sensor designs obtained from this work include an exclusive phenol sensor (MopR$^{AB}_{HN}$), *ortho*-phenol sensor (MopR$^{AB}_{WA}$), *meta*-phenol sensor (MopR$^{AB}_{HA}$), xylenol sensor (MopR$^{AB}_{WHA}$), and catechol sensor (MopR$^{AB}_{HY}$) (Figure 5C−G). An advantage of this work is that the ligand binding pocket of the same template protein can be engineered according to the target requirements, which makes it an economical and efficient approach. At present, our tested selective biosensors can sense the contaminants below the estimated risk limits as per OSHA. In order to achieve even higher sensitivity of these selective sensors for pollutant detection, further efforts are underway toward construction and quantitative detection of these

DOI: 10.1021/acssensors.6b00843
ACS Sens. XXXX, XXX, XXX−XXX

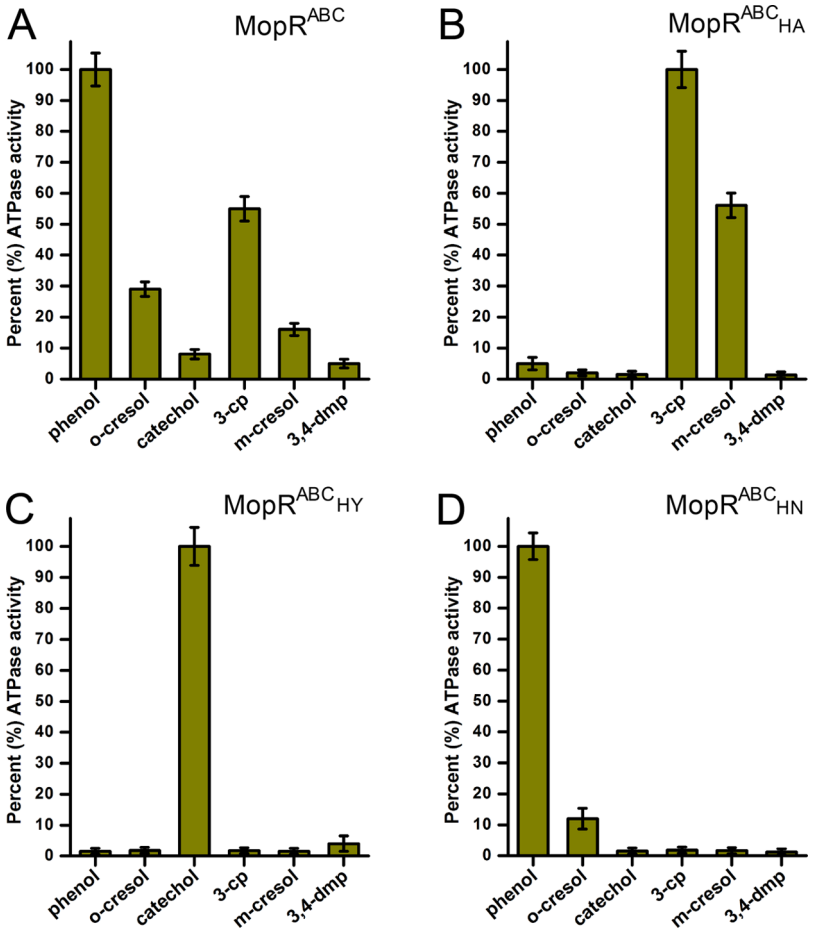

Figure 6. Translational biosensing ability of various selective sensor designs of MopR. Panels represent percent (%) ATPase activity of native (A) and mutated (B–D) MopR^{ABC} constructs (comprising the pollutant sensing (A) and readout ATPase (C) domain) toward select pollutants, tested using a colorimetric ATPase assay.[26]

aromatic pollutants from real time environmental samples. This study is a stepping stone toward efficient bioremediation of target aromatic pollutants.

■ ASSOCIATED CONTENT

Supporting Information

The Supporting Information is available free of charge on the ACS Publications website at DOI: 10.1021/acssensors.6b00843.

Supporting Materials and Methods, supporting references, binding analysis of MopR$^{AB}_{HA}$, MopR$^{AB}_{WA}$, MopR$^{AB}_{HY}$, MopR$^{AB}_{WHA}$, structure guided sensing of xylenols, affinity of MopR$^{AB}_{HN}$ toward different phenol derivatives, docking of MopR^{AB} mutants, thermodynamic parameters of MopR^{AB} mutants (PDF)

■ AUTHOR INFORMATION

Corresponding Author

*E-mail: ruchi@chem.iitb.ac.in.

ORCID

Ruchi Anand: 0000-0002-2045-3758

Author Contributions

S.R., S.P., and R.A. designed research; S.R. performed research; R.A. contributed new reagents/analytic tools; S.R., S.P., and R.A. analyzed data; and S.R., S.P., and R.A. wrote the paper.

Notes

The authors declare no competing financial interest.

■ ACKNOWLEDGMENTS

This work was funded by DST, Government of India (Grant Numbers EMR/2015/002121 and DST/TM/WTI/2K16/252) and Australia-India Council(AIC) grant.

■ REFERENCES

(1) Keith, L. H. The Source of U.S. EPA's Sixteen PAH Priority Pollutants. *Polycyclic Aromat. Compd.* **2015**, *35*, 147–160.

(2) Golovleva, L. A.; Aharonson, N.; Greenhalgh, R.; Sethunathian, N.; Vonk, J. W. The role and limitations of microorganisms, in the conversion of xenobiotics (IUPAC reports on pesticides no. 27). *Pure Appl. Chem.* **1990**, *62* (2), 351–364.

(3) Abdel-Shafy, H. I.; Mansour, M. S. M. A review on polycyclic aromatic hydrocarbons: Source, environmental impact, effect on human health and remediation. *Egypt. J. Pet.* **2016**, *25* (1), 107–123.

(4) Mahugo Santana, C.; Sosa Ferrera, Z.; Esther Torres Padrón, M.; Juan Santana Rodríguez, J. Methodologies for the extraction of phenolic compounds from environmental samples: new approaches. *Molecules* **2009**, *14* (1), 298–320.

(5) Wille, K.; De Brabander, H. F.; Vanhaecke, L.; De Wulf, E.; Van Caeter, P.; Janssen, C. R. Coupled chromatographic and mass-spectrometric techniques for the analysis of emerging pollutants in the aquatic environment. *TrAC, Trends Anal. Chem.* **2012**, *35*, 87–108.

DOI: 10.1021/acssensors.6b00843
ACS Sens. XXXX, XXX, XXX–XXX

(6) Shingler, V. Integrated regulation in response to aromatic compounds: from signal sensing to attractive behaviour. *Environ. Microbiol.* **2003**, *5* (12), 1226−1241.
(7) Diaz, E.; Prieto, M. A. Bacterial promoters triggering biodegradation of aromatic pollutants. *Curr. Opin. Biotechnol.* **2000**, *11* (5), 467−75.
(8) Timmis, K. N.; Pieper, D. H. Bacteria designed for bioremediation. *Trends Biotechnol.* **1999**, *17* (5), 201−204.
(9) Tropel, D.; van der Meer, J. R. Bacterial transcriptional regulators for degradation pathways of aromatic compounds. *Microbiol. Mol. Biol. Rev.* **2004**, *68* (3), 474−500.
(10) Gerischer, U. Specific and global regulation of genes associated with the degradation of aromatic compounds in bacteria. *J. Mol. Microbiol. Biotechnol.* **2002**, *4* (2), 111−121.
(11) Worsey, M. J.; Franklin, F. C.; Williams, P. A. Regulation of the degradative pathway enzymes coded for by the TOL plasmid (pWWO) from Pseudomonas putida mt-2. *J. Bacteriol.* **1978**, *134* (3), 757−764.
(12) Shingler, V. Signal sensing by σ54-dependent regulators: derepression as a control mechanism. *Mol. Microbiol.* **1996**, *19* (3), 409−416.
(13) North, A. K.; Klose, K. E.; Stedman, K. M.; Kustu, S. Prokaryotic enhancer-binding proteins reflect eukaryote-like modularity: the puzzle of nitrogen regulatory protein C. *J. Bacteriol.* **1993**, *175* (14), 4267−4273.
(14) Bush, M.; Dixon, R. The Role of Bacterial Enhancer Binding Proteins as Specialized Activators of σ(54)-Dependent Transcription. *Microbiol. Mol. Biol. Rev.* **2012**, *76* (3), 497−529.
(15) Wootton, J. C.; Drummond, M. H. The Q-linker: a class of interdomain sequences found in bacterial multidomain regulatory proteins. *Protein Eng., Des. Sel.* **1989**, *2*, 535−543.
(16) O'Neill, E.; Ng, L. C.; Sze, C. C.; Shingler, V. Aromatic ligand binding and intramolecular signalling of the phenol-responsive σ54-dependent regulator DmpR. *Mol. Microbiol.* **1998**, *28* (1), 131−141.
(17) Ng, L. C.; O'Neill, E.; Shingler, V. Genetic Evidence for Interdomain Regulation of the Phenol-responsive 54-dependent Activator DmpR. *J. Biol. Chem.* **1996**, *271* (29), 17281−17286.
(18) Kim, M. N.; Park, H. H.; Lim, W. K.; Shin, H. J. Construction and comparison of Escherichia coli whole-cell biosensors capable of detecting aromatic compounds. *J. Microbiol. Methods* **2005**, *60* (2), 235−245.
(19) Gupta, S.; Saxena, M.; Saini, N.; Mahmooduzzafar; Kumar, R.; Kumar, A. An effective strategy for a whole-cell biosensor based on putative effector interaction site of the regulatory DmpR protein. *PLoS One* **2012**, *7* (8), e43527.
(20) Skärfstad, E.; O'Neill, E.; Garmendia, J.; Shingler, V. Identification of an Effector Specificity Subregion within the Aromatic-Responsive Regulators DmpR and XylR by DNA Shuffling. *J. Bacteriol.* **2000**, *182* (11), 3008−3016.
(21) Devos, D.; Garmendia, J.; Lorenzo, V. d.; Valencia, A. Deciphering the action of aromatic effectors on the prokaryotic enhancer-binding protein XylR: a structural model of its N-terminal domain. *Environ. Microbiol.* **2002**, *4* (1), 29−41.
(22) Ray, S.; Gunzburg, M. J.; Wilce, M.; Panjikar, S.; Anand, R. Structural Basis of Selective Aromatic Pollutant Sensing by the Effector Binding Domain of MopR, an NtrC Family Transcriptional Regulator. *ACS Chem. Biol.* **2016**, *11* (8), 2357−2365.
(23) Patil, V. V.; Park, K. H.; Lee, S. G.; Woo, E. Structural Analysis of the Phenol-Responsive Sensory Domain of the Transcription Activator PoxR. *Structure* **2016**, *24* (4), 624−30.
(24) Turnbull, A. P.; Kümmel, D.; Prinz, B.; Holz, C.; Schultchen, J.; Lang, C.; Niesen, F. H.; Hofmann, K.-P.; Delbrück, H.; Behlke, J.; Müller, E.-C.; Jarosch, E.; Sommer, T.; Heinemann, U. Structure of palmitoylated BET3: insights into TRAPP complex assembly and membrane localization. *EMBO J.* **2005**, *24* (5), 875−884.
(25) Morris, G. M.; Huey, R.; Lindstrom, W.; Sanner, M. F.; Belew, R. K.; Goodsell, D. S.; Olson, A. J. AutoDock4 and AutoDockTools4: Automated docking with selective receptor flexibility. *J. Comput. Chem.* **2009**, *30* (16), 2785−91.
(26) Baykov, A. A.; Evtushenko, O. A.; Avaeva, S. M. A malachite green procedure for orthophosphate determination and its use in alkaline phosphatase-based enzyme immunoassay. *Anal. Biochem.* **1988**, *171* (2), 266−70.

DOI: 10.1021/acssensors.6b00843
ACS Sens. XXXX, XXX, XXX−XXX